^{15}N Solid-State NMR Characterization of Ammonia Adsorption Environments in 3A Zeolite Molecular Sieves

G. P. Holland,* B. R. Cherry, and T. M. Alam

Department of Biomolecular and Chemical Analysis, Sandia National Laboratories, Albuquerque, New Mexico 87185

Received: May 17, 2004; In Final Form: August 12, 2004

The quantitative analysis of ammonia binding sites in 3A zeolite molecular sieves using solid-state ^{15}N MAS NMR spectroscopy is reported. By utilizing ^{15}N-enriched ammonia ($^{15}NH_3$) gas, the different adsorption/binding sites within the zeolite were characterized as a function of NH_3 loading. Using ^{15}N MAS NMR, multiple sites were resolved that have distinct cross-polarization dynamics, relaxation, and chemical shift behavior. A combination of $^{15}N/^{23}Na$ and $^{15}N/^{27}Al$ TRAPDOR NMR methods was used to demonstrate significant dipolar coupling between adsorbed ammonia molecules and both Na cations and Al framework species in the zeolite cage. An estimate of the $^{23}Na-^{15}N$ and $^{27}Al-^{15}N$ distance was obtained from simulation of the TRAPDOR results. Two-dimensional $^1H \rightarrow {}^{15}N$ CP-MAS NMR exchange spectroscopy was implemented to probe dynamics between the two primary adsorbed ammonia environments. In the 3A zeolite, the observed exchange process between the ammonia sites does not display a significant temperature dependence, indicating a spin-diffusion mechanism.

Introduction

Zeolites are extensively used in a wide variety of applications including catalysis, gas separation, and as drying agents.[1−3] Small molecules will adsorb in the cagelike structures of these aluminosilicate materials if the adsorbate has a critical diameter smaller than the pore size of the zeolite. Varying the cations present in the cage can control this pore size.[2] In the case of zeolite A molecular sieves (which are typically used as drying agents) the Na form has a pore size of ∼4 Å while the K-exchanged material has a ∼3 Å pore diameter. The crystal structures[4] and physical properties[5] of zeolite A molecular sieves have been known for decades; however, the local environment of adsorbed species is still not well understood, particularly for the 3A (K-exchanged) molecular sieve.

Solid-state ^{15}N NMR spectroscopy has been successfully employed in the study of adsorption environments on solid surfaces.[6−15] Enriched NH_3 and N_2 gas have been implemented to quantitatively study the adsorption sites in various zeolites.[6,7,10] The ^{15}N chemical shift is a valuable tool for distinguishing between complexes, binding environments, and gaseous and even liquid environments in the zeolite cage.[6,7,10] Further information regarding Lewis and Brønsted acidity can also be determined from ^{15}N NMR data.[9,11,13,14]

Structural details regarding the proximity between adsorbed molecules and framework species can be explored using TRAPDOR (transfer of populations in double resonance) NMR techniques. These TRAPDOR NMR experiments detect dipolar couplings between spin-$^1/_2$ and quadrupolar ($I > {}^1/_2$) nuclei.[16,17] For example, $^1H/^{27}Al$ TRAPDOR NMR has been employed to detect and measure large ^{27}Al quadrupole coupling constants in dehydrated zeolite HY,[18] while $^{15}N/^{27}Al$ TRAPDOR experiments performed at low temperatures showed that monomethylamine was adsorbed near ^{27}Al surface sites in the HY material.[13,19]

Dynamic processes between different chemical environments can be studied with two-dimensional (2D) exchange NMR.[20,21] Exchange experiments have been previously used to observe hopping processes of adsorbed species between various sites in zeolitic systems.[22−24] In the case of a faujasite-type Ca-LSX zeolite, ^{13}C 2D exchange NMR detected hopping of adsorbed benzene molecules between different Ca^{2+} cation adsorption sites. Measurements performed at different temperatures revealed the activation barrier for benzene hopping.[23] In a similar fashion, Fyfe and co-workers utilized ^{13}C 2D exchange NMR to obtain activation barriers for *p*-xylene motions in both the zigzag and straight channels of ZSM-5 zeolite.[24]

In the present study a combination of solid-state NMR methods is implemented to characterize the ammonia adsorption sites in 3A zeolite molecular sieves. Solid-state ^{15}N magic angle spinning (MAS) NMR spectroscopy is used to directly determine the concentrations of distinct adsorption/binding sites in the 3A zeolite. The proximity between adsorbed ammonia molecules and both Na cations and Al framework species in the zeolite cage is extracted from $^{15}N/^{23}Na$ and $^{15}N/^{27}Al$ TRAPDOR measurements, respectively. Finally, ^{15}N 2D exchange spectroscopy is utilized to probe the dynamics between distinct ammonia adsorption environments.

Experimental Section

Activation of the Type 3A molecular sieve (Davison, St. Louis, MO), having a nominal chemical formula of $Na_{6.6}K_{5.4}$-$[(AlO_2)_{12}(SiO_2)_{12}]$, was achieved by drying the samples at 176 °C under vacuum for 48 h. The samples were immediately transferred from the oven to a nitrogen-filled glovebox to avoid moisture contamination. Approximately 300 mg of the activated zeolite was packed and sealed in Swagelok stainless steel containers in the glovebox. The sealed samples were evacuated (10^{-5} Torr) and exposed to a given pressure (100−700 Torr) of ^{15}N-labeled ammonia gas (99%, Cambridge Isotopes). The system was allowed to equilibrate to some final pressure after

* Corresponding author: e-mail gpholla@sandia.gov.

10.1021/jp047884j CCC: $27.50
Published on Web 09/25/2004

2−5 h. The total amount of adsorbed gas was calculated from the initial and final pressures, implementing the ideal gas law. Ammonia loading is expressed in mmol of ammonia per gram of activated molecular sieve.

The solid-state ^{15}N MAS NMR spectra were obtained at a resonance frequency of 40.55 MHz on a Bruker Avance400 NMR spectrometer using a 7 mm cross-polarization (CP)-MAS probe spinning at 5 kHz. Typical ^{15}N MAS NMR conditions for direct polarization (DP) experiments used an 8.5 μs $\pi/2$ pulse, 170 s recycle delay, and 128 scan averages. This recycle delay is greater than $5T_1$, allowing for accurate quantification of the different resonances. The ^{15}N CP-MAS NMR spectra were obtained using 1024 scans, an 8.5 μs ^{1}H $\pi/2$ pulse, a 4.5 ms contact pulse, and a 2 s recycle delay. Two pulse phase modulation (TPPM) ^{1}H decoupling was applied during acquisition in both DP and CP experiments.[25] The ^{15}N NMR spectra were referenced to nitromethane ($\delta = 0.0$ ppm) by calibrating to a secondary standard of ^{15}N-labeled glycine ($\delta = -347.6$ ppm). Spin−lattice (T_1) relaxation measurements were performed with the saturation recovery method.[26] Spectral deconvolutions of the observed NMR resonances were performed using the DMFIT program.[27]

The ^{15}N/^{23}Na and ^{15}N/^{27}Al TRAPDOR experiments utilized a 4 mm triple-resonance Bruker MAS probe operating at 400.15, 105.85, 104.27, and 40.55 MHz for ^{1}H, ^{23}Na, ^{27}Al, and ^{15}N, respectively. CP was applied in all TRAPDOR experiments with the same parameters as discussed above. The TRAPDOR sequence was performed as previously described where a rotor synchronized spin echo is applied with and without ^{23}Na/^{27}Al RF irradiation during the first half of the echo sequence.[17] The experiment executed without RF irradiation provides a reference spectrum (S_0) that compensates for echo decay resulting from spin−spin relaxation (T_2). A MAS frequency of 1 kHz was implemented to ensure adiabatic population transfer between the ^{23}Na and/or ^{27}Al ($I > 1/2$) and the ^{15}N ($I = 1/2$) nuclei. The ^{23}Na and ^{27}Al RF field strength utilized was 71 kHz. Simulations of the TRAPDOR experiments were performed with the SIMPSON software package.[28]

^{15}N 2D exchange NMR was applied as previously discussed where the CP pulse sequence is used with a variable evolution period and a fixed mixing time to monitor exchange.[20] The mixing time (τ_m) was varied between 200 μs and 2 s, and data were collected at different temperatures (298−373 K). The sweep width was 5 kHz in both dimensions, and 256 t_1 points were collected. ^{1}H decoupling was not applied during τ_m.

Results and Discussion

The solid-state DP ^{15}N MAS NMR spectra for the 3A zeolite molecular sieve as a function of ammonia loading are shown in Figure 1. Up to five distinct ^{15}N resonances (I−V) are observed (see inset). Two primary resonances (labeled I and II) comprise a minimum of 85% of the total observed signal. The concentrations, chemical shifts, and line widths of the different environments are listed in Table 1. The concentrations were obtained on the basis of relative peak intensities and the total ammonia concentration. This paper will focus on understanding the origin of resonances I and II since they represent the vast majority of the ammonia adsorption sites in this material (>85%).

The variation in the concentration of adsorption sites I and II as a function of loading is shown in Figure 2. The ^{15}N species giving rise to resonance I appear to populate first since this resonance dominates the spectrum (see Figure 1) at the lowest loading of 0.35 mmol/g (~80% of the total intensity). This

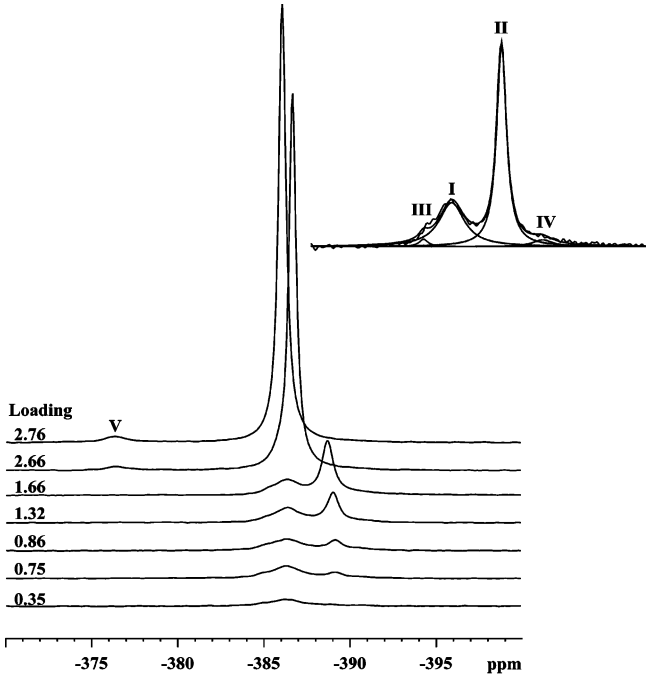

Figure 1. ^{15}N DP MAS NMR of 3A zeolite as a function of ammonia loading. Loading in mmol/g is indicated in the figure. A deconvoluted spectrum of the sample with an ammonia loading of 1.66 mmol/g is shown in the inset.

adsorption environment saturates at a loading of 1.32 mmol/g, while the concentration of resonance II increases continuously (see Figure 2) as the ammonia loading is increased.

The two resonances display different chemical shift behavior as a function loading, as shown in Figure 3. Resonance I exhibits a constant chemical shift of ~−386.4 ppm across the entire ammonia loading range studied, while resonance II displays an increased chemical shift when the number of adsorbed ammonia molecules per α-cage (N) is increased beyond unity. The latter behavior has been observed previously in the ^{15}N MAS NMR spectra of adsorbed ammonia in various zeolitic materials and was unambiguously attributed to a close packing of the ammonia molecules in the α-cage, resulting in a shift toward that of liquid ammonia (−381.9 ppm).[6,7] This indicates that resonance II interacts closely with other ammonia molecules as the loading is increased presumably through formation of hydrogen-bonded networks in the zeolite cage. The constant chemical shift observed for resonance I suggests that this ammonia site does not experience a liquidlike environment or participate in hydrogen bonding with other adsorbed ammonia molecules. It should be noted that at the highest loading studied (4.0 mmol/g) resonance I does display a minor shift (~0.5 ppm) toward liquid ammonia.

Differences in dynamic behavior between ammonia environments can be obtained from relaxation measurements. Spin−lattice (T_1) relaxation times were measured for the two principal ammonia environments (I and II). Saturation recovery profiles are depicted in Figure 4 for the zeolite sample containing 1.66 mmol of ammonia per gram of activated zeolite. Resonance II has a significantly shorter T_1 relaxation time of 4 s compared to 34 s observed for resonance I. In the slow-motion regime, the T_1 relaxation time will increase as the motional correlation time decreases; therefore, these differences in T_1 can be interpreted as resulting from differences in mobility between the two ammonia environments. The longer relaxation time measured for resonance I suggests a more rigid ammonia environment, while resonance II is characteristic of a more

TABLE 1: ^{15}N Chemical Shift (δ) in ppm, Concentration, and Line Width of Different Ammonia Sites Obtained from ^{15}N MAS NMR Spectra of $^{15}NH_3$ in 3A Zeolite

site	I			II			III		IV		V	
loading[a]	δ	concn[b]	fwhm[c]	δ	concn	fwhm	δ	concn	δ	concn	δ	concn
0.35	−386.4	0.27	101	−388.8	0.03	-	−385.0	0.04	−390.7	0.01	-	-
0.75	−386.3	0.58	87	−389.2	0.11	49	−385.1	0.02	−390.6	0.03	-	-
0.86	−386.4	0.56	92	−389.1	0.22	46	−385.1	0.05	−390.6	0.03	-	-
1.32	−386.4	0.69	79	−389.1	0.60	34	−385.1	0.02	−390.6	0.02	-	-
1.66	−386.4	0.56	70	−388.7	1.06	33	−385.1	0.04	−390.6	-	-	-
2.66	−386.4	0.46	-	−386.7	2.05	21	−385.1	0.06	−390.6	-	−376.5	0.09
2.76	−386.4	-	-	−386.1	2.46	21	−385.1	-	−390.6	-	−376.4	0.10
4.0	−385.7	0.06	26	−382.6	3.44	12	-	-	-	-	−376.5	0.50

[a] Loading in mmol of NH_3 per gram of activated zeolite. [b] Concentration given by mmol species per gram of activated zeolite. [c] Full width at half-maximum (fwhm) in Hz.

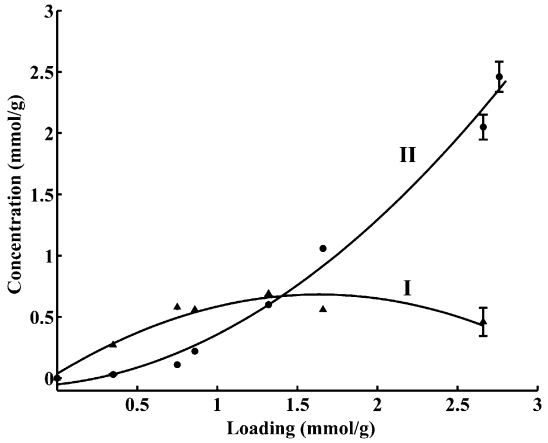

Figure 2. Concentration of the two primary adsorption environments, site I (▲) and site II (●), as a function of ammonia loading.

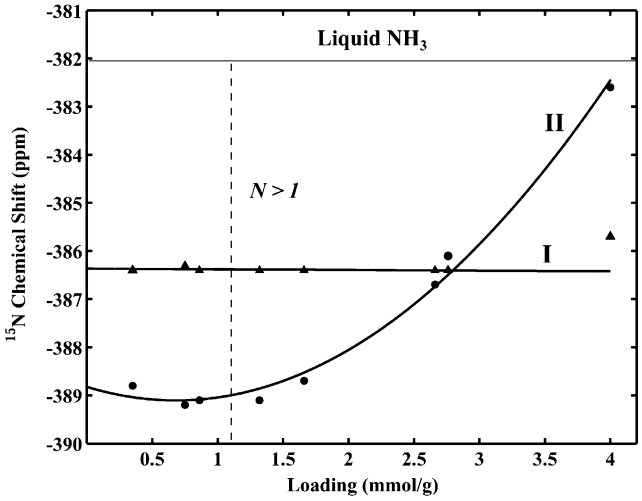

Figure 3. ^{15}N chemical shift of the two primary adsorption environments, site I (▲) and II (●), as a function of ammonia loading. *N* indicates the number of adsorbed ammonia molecules per α-cage.

dynamic environment. This is consistent with the chemical shift results, which indicated that resonance II becomes liquidlike or more dynamic as the ammonia concentration is increased. The full width at half-maximum (fwhm) decreases for both species as the ammonia doping is increased, which is also consistent with an increased mobility (see Table 1).

The solid-state $^1H \rightarrow {}^{15}N$ CP-MAS NMR spectra for the 3A zeolite as a function of ammonia loading are shown in Figure 5. Similar environments are resolved compared to the DP experiments depicted in Figure 1, but differences in relative intensities are observed. Resonance I displays a more intense signal than resonance II and, therefore, is more effectively cross-

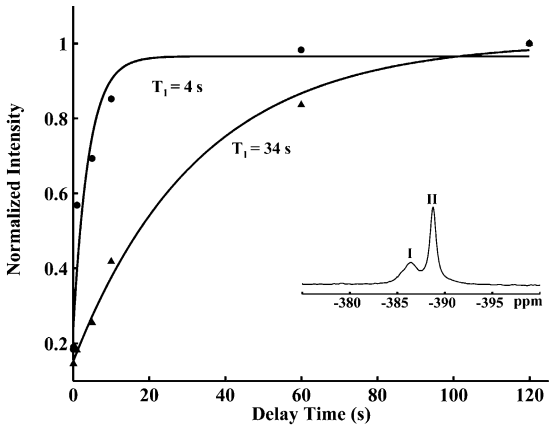

Figure 4. Saturation recovery profiles for the sample with a loading of 1.66 mmol/g. The T_1 measured for the two primary ammonia adsorption environments, site I (▲) and site II (●), are indicated in the figure.

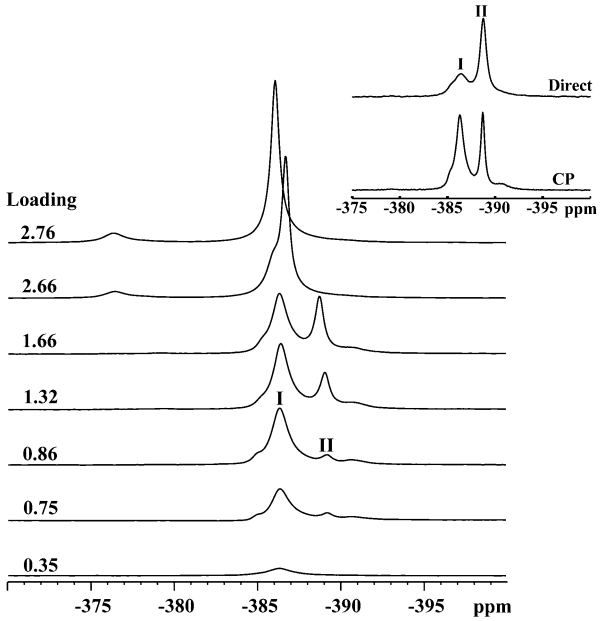

Figure 5. ^{15}N CP-MAS NMR of 3A zeolite as a function of ammonia loading with a 4.5 ms contact time. Loading in mmol/g is indicated in the figure.

polarized by neighboring protons. The DP and CP spectrum of the sample containing 1.32 mmol/g is displayed in the inset of Figure 5 for comparison purposes. These differences in CP efficiency characteristically indicate differences in mobility between the two environments since the proximity of protons is similar. Therefore, resonance I likely corresponds to NH_3 molecules occupying a site that is more strongly bound than

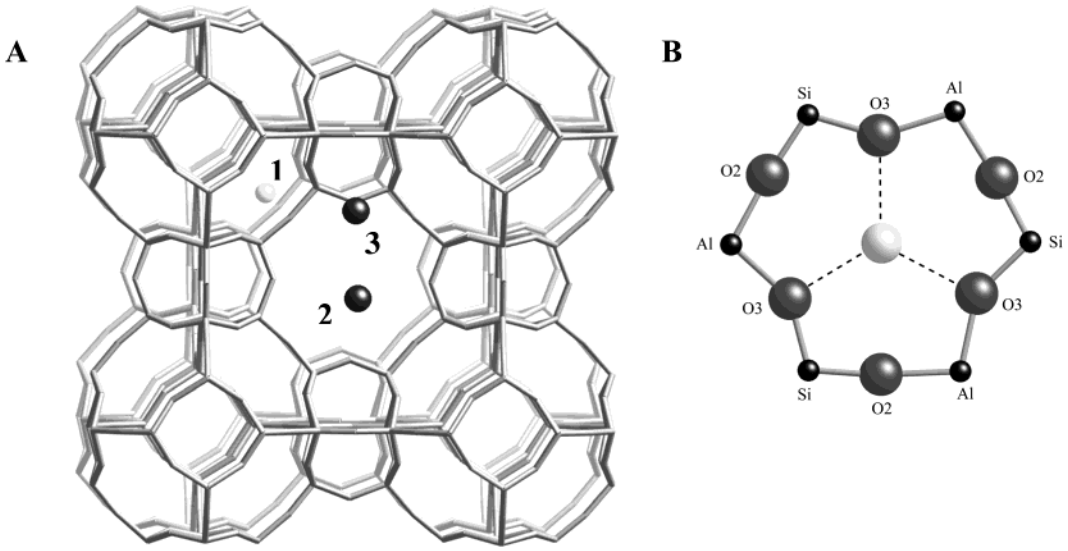

Figure 6. (A) The framework structure and cation sites for zeolite 3A molecular sieve and (B) the Na 6-ring, 3-fold coordination environment. Cation site 1 is occupied primarily by Na while K resides in sites 2 and 3.

those represented by resonance II. On the basis of the chemical shift behavior, CP efficiency, and T_1 relaxation times, we assign resonance I to bound, immobile NH_3 while resonance II corresponds to a more dynamic, liquidlike ammonia environment. This result is similar to a ^{2}H NMR study on phenanthrene-d_{10} adsorbed in zeolites X and Y where a rigid and mobile ^{2}H environment was observed. The rigid environment was shown to be associated with the cation sites while the mobile environment was attributed to dynamic phenanthrene in the supercage.[29]

The framework structure of the 3A zeolite is shown in Figure 6A. The framework is composed of aluminosilicate sodalite cages (β-cage) that arrange to form a larger α-cage with a 3 Å pore opening. There are three cation sites: one in the 6-ring of the β-cage (cation environment 1), one in the 8-ring of the α-cage (cation environment 2), and one near the 4-ring (cation environment 3). The K cations will preferentially occupy sites 2 and 3 due to their larger ionic radius while, the Na cations will remain in site 1.[30] X-ray diffraction experiments previously performed on ammonia adsorbed in zeolite 4A revealed two primary adsorption environments in the α-cage.[31] One involved adsorption to the 3-fold axis Na cations (Figure 6B), and the other represented ammonia molecules which were hydrogen-bonded to these and framework oxygen atoms. On the basis of the results presented here regarding ammonia adsorbed in zeolite 3A, it would seem probable to conclude that resonance I corresponds to NH_3 molecules that are adsorbed to the 3-fold axis cations while resonance II represents those NH_3 species in hydrogen-bonded environments. Considering the chemical shift, relaxation, and CP data, it appears that the ammonia molecules associated with cationic environments are rigidly bound while those in hydrogen-bonded networks are more mobile at room temperature. Unfortunately, the X-ray experiments were unable to distinguish whether the cationic adsorption environments populated first in a partially filled, ammonia sorption complex.[32] However, the ^{15}N MAS results on the lower ammonia loadings presented in Figure 1 clearly indicate that site I populates before site II in the case of zeolite 3A, indicating a preference for the cationic sites.

For the case of a partially K-exchanged, dehydrated zeolite 3A, there is only one Na site reported from the neutron powder diffraction crystal structure where the Na cation resides in the center of a 6-ring with a 3-fold coordination environment (Figure 6B).[30] This coordination environment results in an axially symmetric electric field gradient with $C_Q = 5.8$ MHz and $\eta \approx 0$.[33,34] This was consistent with the ^{23}Na MAS NMR on the dehydrated 3A zeolite sample studied here (data not shown). Only one primary Na site was observed with $C_Q = 6.1$ MHz and $\eta \approx 0$, confirming the Na location within the 6-ring site. Further verification was obtained by moving the ^{23}Na offset frequency and performing the ^{15}N/^{23}Na TRAPDOR experiment (see Figure 7). An estimate of C_Q can be obtained from the cutoff frequency (υ_c) at which the TRAPDOR efficiency drops to zero.[18,35] For a spin-$^3/_2$ nucleus like ^{23}Na, $C_Q = 2\upsilon_c$. The results presented in Figure 7 yield $C_Q \approx 7.0 \pm 0.5$ MHz, in good agreement with the C_Q derived from the ^{23}Na MAS NMR results. This confirms that the primary Na site present is within the 6-ring, 3-fold coordinated and that the ammonia molecules corresponding to resonance I interact with this specific cation environment (see Figure 6B, cation site 1). Na cations occupying 4-ring and 8-ring coordination environments are expected to yield smaller quadrupole coupling constants and larger asymmetry parameters ($C_Q = 3.2$ MHz and $\eta = 0.9$) and were not observed in the 3A material.[34]

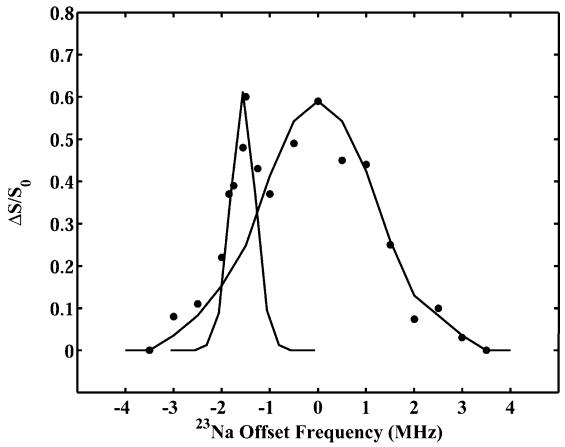

Figure 7. ^{15}N/^{23}Na, ^{27}Al TRAPDOR fraction, $\Delta S/S_0$, as a function of ^{23}Na offset frequency. Simulation was performed with SIMPSON software package, $C_Q = 7.0$ MHz for ^{23}Na and $C_Q = 3.0$ MHz for ^{27}Al, experimental data (●).

To confirm assigning resonance I to a Na cation binding environment, ^{15}N/^{23}Na TRAPDOR experiments were implemented to detect dipolar coupling between the adsorbed

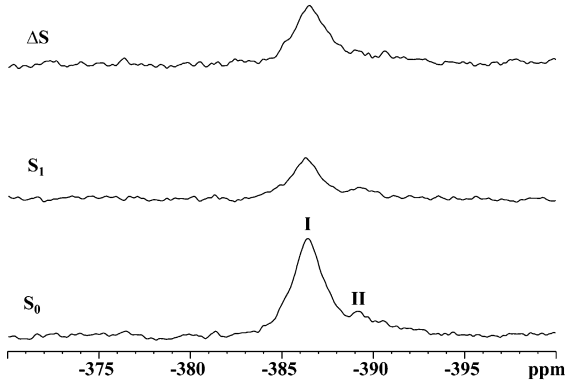

Figure 8. $^{15}N/^{23}Na$ TRAPDOR experiment with ^{23}Na irradiation for five rotor cycles (5 ms) performed on sample with 0.75 mmol/g ammonia loading. Reference spectrum (S_0), TRAPDOR spectrum (S_1), and difference spectrum ($\Delta S = S_0 - S_1$) are indicated in the figure.

ammonia and Na cations. To obtain reliable TRAPDOR results, population transfer between the two nuclei needs to be adiabatic. Vega derived an expression for the adiabaticity, α, of a whole powder distribution:

$$\alpha = \nu_1^2/\nu_Q\nu_r \quad (1)$$

where ν_1, ν_Q, and ν_r are the RF field strength, the quadrupole frequency, and the rotor spinning frequency, respectively.[36] Adiabaticity values greater than unity ensure that the majority of the ^{23}Na passages occur for the entire powder. Using RF field strength of 71 kHz, a quadrupole frequency of 3.5 MHz, and a rotor spinning frequency of 1 kHz, an α value of 1.4 is calculated ensuring primarily adiabatic passages in the $^{15}N/^{23}Na$ TRAPDOR experiments discussed below.

Another consideration regarding $^{15}N/^{23}Na$ TRAPDOR experiments performed as a function of offset frequency are contributions from ^{27}Al. The ^{27}Al (104.229 MHz) and ^{23}Na (105.805 MHz) Larmor frequencies are only separated by 1.576 MHz at the magnetic field strength employed (9.4 T). If the C_Q of ^{27}Al is large enough (>1 MHz), ^{15}N dephasing due to dipolar interactions with ^{27}Al could result. Clearly, when the offset frequency nears the ^{27}Al resonant frequency, a spike in the TRAPDOR effect is observed (see Figure 7), indicating ^{15}N dephasing due to dipolar coupling with ^{27}Al sites. This is similar to observations made previously where a dual contribution from ^{23}Na and ^{27}Al was observed when performing $^{1}H/^{27}Al$ rotational echo adiabatic passage double-resonance (REAPDOR) experiment as a function of ^{27}Al offset frequency on CH_3I adsorbed in NaX zeolite.[37] The simulated data displayed in Figure 7 were calculated utilizing a $C_Q = 7.0$ MHz for ^{23}Na and $C_Q = 3.0$ MHz for ^{27}Al. When the TRAPDOR experiment is performed for an on-resonance ^{23}Na condition, no contribution from ^{27}Al can be assumed; however, for an on-resonance ^{27}Al condition a combination from both ^{27}Al and ^{23}Na will result since the two overlap as shown in Figure 7 (discussed further below).

The $^{15}N/^{23}Na$ TRAPDOR results for a sample with a 0.75 mmol/g loading are depicted in Figure 8. This experiment was performed with a ^{23}Na irradiation time of 5 ms (five rotor cycles). Clearly, a considerable $^{15}N/^{23}Na$ TRAPDOR effect is observed. Resonance I displays a 61% decrease in intensity, confirming that significant dipolar coupling persists between the Na cations and the ^{15}N of adsorbed ammonia. This indicates that these adsorbed ammonia molecules are located within close proximity (<5 Å) of the Na cations. A TRAPDOR effect is also displayed by resonance II which also indicates a proximity to the Na cations. However, the TRAPDOR effect is smaller,

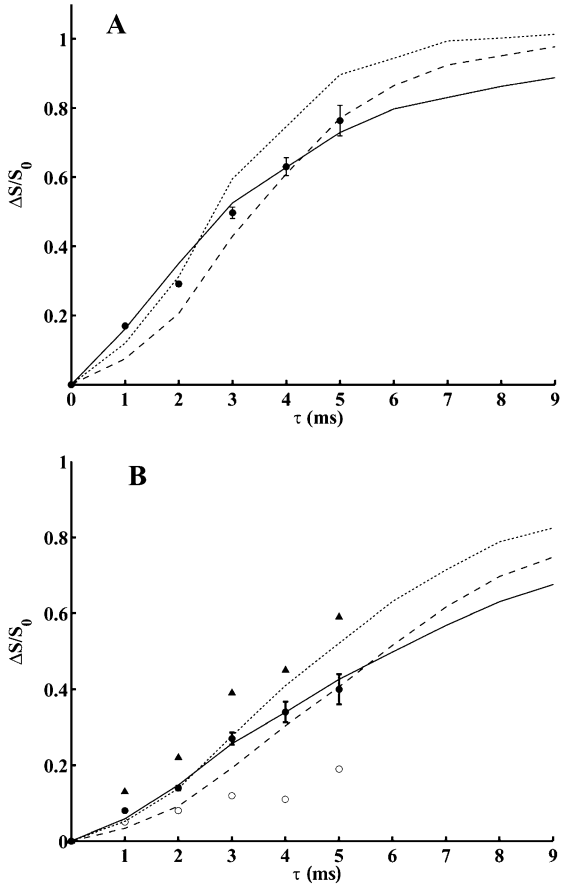

Figure 9. TRAPDOR curves collected as a function of irradiation time (τ) for ^{23}Na (A) and ^{27}Al (B) on-resonance conditions. Simulations performed for ^{23}Na irradiation with $D = 140$ Hz (dotted line), 110 Hz (dashed line), 360 Hz and $\beta = 55°$ (solid line), and experimental data (●). Simulations performed for ^{27}Al with $D = 75$ Hz (dotted line), $D = 60$ Hz (dashed line), and $D = 165$ Hz and $\beta = 55°$ (solid line). The contribution from ^{23}Na was obtained by collecting a TRAPDOR curve at +1.576 MHz from ^{23}Na (○) and subtracting it from the experimental data for ^{27}Al collected on-resonance (▲) to give the difference spectrum (●).

which likely results due to differences in dynamics between the two environments.

The fractional $^{15}N/^{23}Na$ TRAPDOR effect ($\Delta S/S_0$) observed for resonance I is plotted as a function of ^{23}Na irradiation time in Figure 9A. This curve is related to the dipolar coupling (D_{ij}) between the ^{23}Na and ^{15}N nuclei, and the interatomic distance (r_{ij}) can be extracted from the following equation:

$$D_{ij} = \frac{\mu_0 \hbar \gamma_i \gamma_j}{4\pi r_{ij}^3} \quad (2)$$

where γ_i and γ_j are the gyromagnetic ratios of the coupled nuclei. The TRAPDOR curve is sensitive to the orientation of the quadrupolar and dipolar tensors, which are typically not known.[38] In Figure 9A simulations performed with the tensors collinear yielded a $^{15}N/^{23}Na$ dipolar coupling between 110 and 140 Hz. When the angle β is changed to 55° (near the magic angle), a much larger dipolar coupling of 360 Hz is necessitated to fit the curve. This difficulty when fitting TRAPDOR curves has been discussed previously with regards to $^{31}P/^{27}Al$ TRAPDOR experiments on trimethylphosphine adsorbed in zeolite HY.[39] Nonetheless, these TRAPDOR experiments provide an estimate of the distance, and we can conclude that the distance between the Na cation in the 6-ring and the N of the ammonia

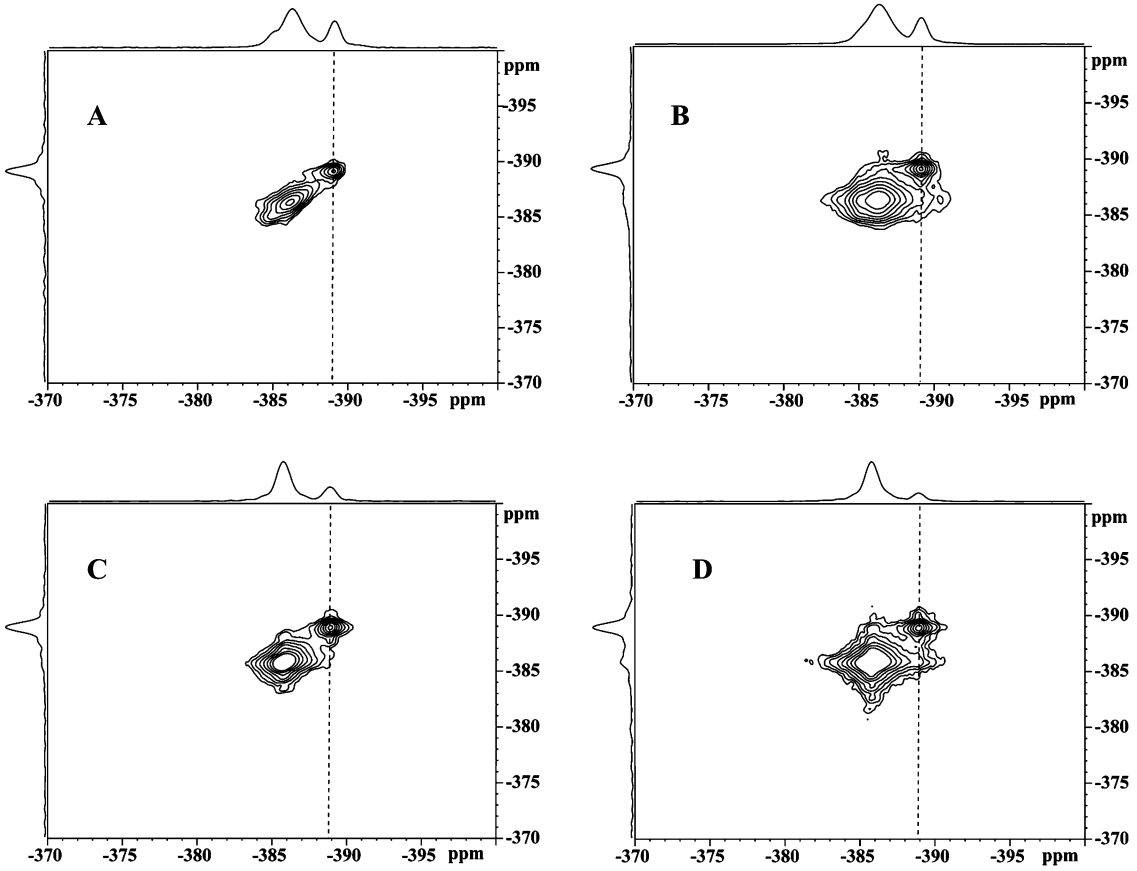

Figure 10. 2D ^{15}N CP-MAS exchange spectrum for sample with 0.86 mmol/g at (A) 295 K with $\tau_m = 200$ μs, (B) 295 K with $\tau_m = 500$ ms, (C) 373 K with $\tau_m = 200$ μs, and (D) 373 K with $\tau_m = 500$ ms. The dashed line indicates where the vertical projected slice was taken.

molecule is between 2.1 and 3.1 Å. This short distance indicates a strong electrostatic interaction between the loan pair on the N of the adsorbed ammonia molecule and the Na cation. This distance range is consistent with the Na−N distances measured by XRD on ammonia adsorbed in zeolite 4A where the two ammonia environments in the α-cage were located 2.2 and 2.9 Å from the Na cation.[31] TRAPDOR experiments were also conducted at −50 °C, ensuring that resonance I was not impacted by dynamics. The TRAPDOR buildup curve obtained was identical to that collected at room temperature, showing that this environment is completely rigid at room temperature.

The fractional ^{15}N/^{27}Al TRAPDOR effect ($\Delta S/S_0$) observed for resonance I as a function of ^{27}Al irradiation time is displayed in Figure 9B. For an on-resonance ^{27}Al condition contributions from ^{23}Na must be considered since the two quadrupole frequencies overlap as shown in Figure 7. To obtain an estimate of the contribution from ^{23}Na dipolar coupling during ^{27}Al irradiation, a TRAPDOR curve was collected +1.576 MHz from ^{23}Na (outside the frequency of the ^{15}N−^{27}Al coupling, see Figure 7). Since the quadrupole frequency is symmetric about the on-resonance condition, this will provide a good estimate of the contribution from Na during on-resonance ^{27}Al irradiation (−1.576 MHz from ^{23}Na). The contribution from ^{23}Na was subtracted from the curve obtained with on-resonance ^{27}Al irradiation, providing the sole contribution from ^{27}Al. Again, tensor orientations can impact the measured dipolar coupling as discussed above. A dipolar coupling between 60 and 75 Hz was extracted from the simulations with the tensors collinear, while a value of 165 Hz was obtained from the simulation performed with $\beta = 55°$. The distance between ammonia and ^{27}Al is, therefore, between 2.7 and 3.8 Å using eq 2. Techniques that are not as sensitive to the orientation of the quadrupolar and dipolar tensors like REAPDOR[40] are currently being pursued in our laboratory to obtain more accurate distances.

The dynamics of the ammonia environments in the 3A zeolite cage were also explored with 2D ^{15}N exchange spectroscopy. An experiment performed on a sample with 0.86 mmol/g at 295 K with $\tau_m = 200$ μs (A) and 500 ms (B) is shown in Figure 10. The 2D contour plot of the experiment run with $\tau_m = 200$ μs (A) has predominantly diagonal components, and essentially no spin exchange is observed. In contrast, the 2D exchange NMR spectrum with $\tau_m = 500$ ms (B) demonstrates cross-peaks characteristic of exchange. Similar observations were made for contour plots collected at 373 K (Figure 10C, D). Experiments were run at multiple temperatures (295−373 K), and rate constants (k) were extracted from the following equation as previously described:[24]

$$\ln\left[\frac{I_{S_I S_{II}}(\tau_m) + I_{S_{II} S_{II}}(\tau_m)}{I_{S_I S_{II}}(\tau_m) - I_{S_{II} S_{II}}(\tau_m)}\right] = k\tau_m \qquad (3)$$

where $I_{S_I S_{II}}(\tau_m)$ and $I_{S_{II} S_{II}}(\tau_m)$ are the integrated peak intensities as a function of mixing time for the off-diagonal and diagonal peaks, respectively. The rate constant was relatively consistent across the entire temperature range with $k = 2 \pm 1$ s^{-1}. The fact that the rate constant lacks a temperature dependence indicates that there is no chemical exchange between the two environments at these temperatures. It can be concluded that the cross-peaks observed in Figure 10 result primarily from a spin-diffusion mechanism since chemical exchange is thermally activated, while spin diffusion is typically temperature independent.[23] It is likely that this spin diffusion persists through the proton dipolar coupling. In the current study proton

decoupling was not implemented due to the long exchange mixing periods utilized.

Conclusions

It has been demonstrated that ^{15}N MAS NMR can be used to elucidate multiple NH_3 adsorption environments in 3A zeolite molecular sieves. These ^{15}N MAS NMR experiments show that there are at least 4−5 distinct adsorption sites present in the 3A zeolite. However, site populations are dominated by two primary environments. The primary sites are assigned on the basis of chemical shift, CP behavior, and T_1 relaxation times to rigidly bound ammonia and dynamic ammonia environments in the zeolite α-cage. The $^{15}N/^{23}Na$ TRAPDOR experiments show that the rigid ammonia is adsorbed near the Na cations in the 6-ring and $^{23}Na-^{15}N$ and $^{27}Al-^{15}N$ distances could be estimated from the TRAPDOR results by performing simulations. Two-dimensional NMR exchange spectroscopy displayed cross-peaks indicating an exchange process between the two environments. The exchange process is not a thermally activated chemical exchange but believed to occur via a spin-diffusion mechanism since essentially no temperature dependence was observed.

Acknowledgment. Sandia is a multiprogram laboratory operated by Sandia Corp., a Lockheed Martin Co., for the United States Department of Energy's National Nuclear Security Administration under Contract DE-AC04-94AL85000. This work was funded under the ESC program at Sandia National Laboratories.

References and Notes

(1) Breck, D. W. *Zeolite Molecular Sieves: Structure, Chemistry and Use*; John Wiley & Sons: New York, 1974.
(2) Dyer, A. *An Introduction to Zeolite Molecular Sieves*; John Wiley & Sons: Chichester, 1988.
(3) Karge, H. G. *Catalysis and Adsorption by Zeolites*; Elsevier: Amsterdam, 1991.
(4) Reed, T. B.; Breck, D. W. *J. Am. Chem. Soc.* **1956**, *78*, 5972.
(5) Breck, D. W.; Eversole, W. G.; Milton, R. M.; Reed, T. B.; Thomas, T. L. *J. Am. Chem. Soc.* **1956**, *78*, 5963.
(6) Michel, D.; Germanus, A.; Thomas, B. *Z. Phys. Chem. (Leipzig)* **1981**, *262*, 113.
(7) Michel, D.; Germanus, A.; Pfeifer, H. *J. Chem. Soc., Faraday Trans.* **1982**, *78*, 237.
(8) Earl, W. L.; Fritz, P. O.; Gibson, A. A. V.; Lunsford, J. H. *J. Phys. Chem.* **1987**, *91*, 2091.
(9) Farcasiu, D.; Leu, R.; Corma, A. *J. Phys. Chem. B* **2002**, *106*, 928.
(10) Fonseca, A.; Lledos, B.; Pullumbi, P.; Liginières, J.; Nagy, J. B. *Porous Mater. Environ. Friendly Processes* **1999**, *125*, 229.
(11) Haw, J. F.; Chuang, I.; Hawkins, B. L.; Maciel, G. E. *J. Am. Chem. Soc.* **1983**, *105*, 7206.
(12) Jünger, I.; Meiler, W.; Pfeifer, H. *Zeolites* **1982**, *2*, 310.
(13) Kao, H. M.; Grey, C. P. *J. Phys. Chem.* **1996**, *100*, 5105.
(14) Ripmeester, J. A. *J. Am. Chem. Soc.* **1983**, *105*, 2925.
(15) Jones, C. A.; Stec, D.; Larsen, S. C. *J. Mol. Catal. A* **2004**, *212*, 329.
(16) Grey, C. P.; Veeman, W. S. *Chem. Phys. Lett.* **1992**, *192*, 379.
(17) Grey, C. P.; Veeman, W. S.; Vega, A. J. *J. Chem. Phys.* **1993**, *98*, 7711.
(18) Grey, C. P.; Vega, A. J. *J. Am. Chem. Soc.* **1995**, *117*, 8232.
(19) Grey, C. P.; Kumar, B. S. A. *J. Am. Chem. Soc.* **1995**, *117*, 9071.
(20) Szeverenyi, N. M.; Sullivan, M. J.; Maciel, G. E. *J. Magn. Reson.* **1982**, *47*, 462.
(21) Blümich, B.; Spiess, H. W. *Angew. Chem., Int. Ed. Engl.* **1988**, *27*, 1655.
(22) Larsen, R. G.; Shore, J.; Schmidt-Rohr, K.; Emsley, L.; Long, H.; Pines, A.; Janicke, M.; Chmelka, B. F. *Chem. Phys. Lett.* **1993**, *214*, 220.
(23) Schaefer, D. J.; Favre, D. E.; Wilhelm, M.; Weigel, S. J.; Chmelka, B. F. *J. Am. Chem. Soc.* **1997**, *119*, 9252.
(24) Fyfe, C. A.; Diaz, A. C. *J. Phys. Chem. B* **2002**, *106*, 2261.
(25) Bennett, A. E.; Rienstra, C. M.; Auger, M.; Lakshmi, K. V.; Griffin, R. G. *J. Chem. Phys.* **1995**, *103*, 6951.
(26) Fukushima, E.; Roeder, S. B. *Experimental Pulse NMR*; Perseus Books: Reading, MA, 1981.
(27) Massiot, D.; Fayon, F.; Capron, M.; King, I.; LeCalvé, S.; Alonso, B.; Durand, J.-O.; Bujoli, B.; Gan, Z.; Hoatson, G. *Magn. Reson. Chem.* **2002**, *40*, 70.
(28) Bak, M.; Rasmussen, J. T.; Nielsen, N. C. *J. Magn. Reson.* **2000**, *147*, 296.
(29) Hepp, M. A.; Ramamurthy, V.; Corbin, D. R.; Dybowski, C. *J. Phys. Chem.* **1992**, *96*, 2629.
(30) Adams, J. M.; Haselden, D. A. *J. Solid State Chem.* **1983**, *47*, 123.
(31) Yanagida, R. Y.; Seff, K. *J. Phys. Chem.* **1972**, *76*, 2597.
(32) Yanagida, R. Y.; Seff, K. *J. Phys. Chem.* **1973**, *77*, 138.
(33) Tijink, G. A. H.; Janssen, R.; Veeman, W. S. *J. Am. Chem. Soc.* **1987**, *109*, 7301.
(34) Janssen, R.; Tijink, G. A. H.; Veeman, W. S.; Maesen, T. L. M.; van Lent, J. F. *J. Phys. Chem.* **1989**, *93*, 899.
(35) Zeng, Q.; Nekvasil, H.; Grey, C. P. *J. Phys. Chem. B* **1999**, *103*, 7406.
(36) Vega, A. J. *J. Magn. Reson.* **1992**, *96*, 50.
(37) van Wüllen, L.; Koller, H.; Kalwei, M. *Phys. Chem. Chem. Phys.* **2002**, *4*, 1665.
(38) Kalwei, M.; Koller, H. *Solid State Nucl. Magn. Reson.* **2002**, *21*, 145.
(39) Kao, H. M.; Liu, H.; Jiang, J.; Lin, S. H.; Grey, C. P. *J. Phys. Chem. B* **2000**, *104*, 4923.
(40) Gullion, T. *Chem. Phys. Lett.* **1995**, *246*, 325.